

## Crystal growth and superconductivity of $\text{FeSe}_x$

This article has been downloaded from IOPscience. Please scroll down to see the full text article.

2009 Supercond. Sci. Technol. 22 015020

(<http://iopscience.iop.org/0953-2048/22/1/015020>)

View [the table of contents for this issue](#), or go to the [journal homepage](#) for more

Download details:

IP Address: 202.127.206.173

The article was downloaded on 17/07/2012 at 08:15

Please note that [terms and conditions apply](#).

# Crystal growth and superconductivity of $\text{FeSe}_x$

S B Zhang, Y P Sun<sup>1</sup>, X D Zhu, X B Zhu, B S Wang, G Li, H C Lei, X Luo, Z R Yang, W H Song and J M Dai

Key Laboratory of Materials Physics, Institute of Solid State Physics, Chinese Academy of Sciences, Hefei 230031, People's Republic of China

and

High Magnetic Field Laboratory, Chinese Academy of Sciences, Hefei 230031, People's Republic of China

E-mail: [ypsun@issp.ac.cn](mailto:ypsun@issp.ac.cn)

Received 10 September 2008, in final form 27 October 2008

Published 28 November 2008

Online at [stacks.iop.org/SUST/22/015020](http://stacks.iop.org/SUST/22/015020)

## Abstract

In this work, crystals of  $\text{FeSe}_x$  have been grown by a flux approach. The crystallization process is divided into two stages. First, stoichiometric polycrystal  $\text{FeSe}_{0.82}$  was sintered in a solid state reaction. Then,  $\text{FeSe}_x$  crystals with a size about  $500 \mu\text{m}$  were successfully grown in an evacuated sealed quartz tube using a NaCl/KCl flux. The products include two crystal structures: tetragonal and hexagonal. The electronic transport and magnetic property measurements show that  $\text{FeSe}_x$  crystals exhibit a superconducting transition at about 10 K.

(Some figures in this article are in colour only in the electronic version)

## 1. Introduction

Recently, the discovery of 26 K superconductivity in iron arsenide  $\text{LaO}_{1-x}\text{F}_x\text{FeAs}$  [1] has generated a great deal of interest, and the superconductivity transition temperature  $T_c$  has rapidly been increased to more than 40 K on substituting La by other lanthanides with smaller ionic radius [2–5]. It is supposed that REOFepn (where RE = rare earth; Pn = P, As) is the first system in which the Fe element plays the key role in the occurrence of superconductivity. The parent REOFepn materials possess a simple tetragonal crystal symmetry (ZrCuSiAs-type, space group  $P4/nmm$ ), comprising layers of edge-sharing  $\text{FeAs}_4$  tetrahedra interleaved with RE layers. These discoveries have catalyzed the search for superconducting compositions in related materials in which two-dimensional FeQ (Q = non-metal ions) slabs are also present. The PbO-type structure  $\alpha\text{-FeSe}_{1-x}$  has been reported to have a superconducting transition at about 8 K for  $x = 0.12$  and  $0.18$  [6]. Subsequent work has revealed resistivity onsets for the superconducting transition at a temperature as high as 13.5 K at pressure [7, 8]. FeSe has several phases: (1) a tetragonal phase  $\alpha\text{-FeSe}$  with PbO structure showing a transformation from tetragonal to orthorhombic symmetry

below 70 K at ambient pressure [9]; (2) a NiAs-type  $\beta$  phase with a wide range of homogeneity showing a transformation from hexagonal to monoclinic symmetry; (3) an  $\text{FeSe}_2$  phase which has orthorhombic marcasite structure. (4) Okazaki *et al* have done much detailed research on  $\text{FeSe}_x$  ( $x = 8/7 \sim 4/3$ ). Defects of iron atoms have ordered arrangements in these compounds, and new phases were found in this region. If choose the orthohexagonal and pseudo-orthohexagonal unit cells for  $x = 8/7$  and  $4/3$ , respectively, the unit cell dimensions of the superstructure resulting from this ordering are twice as large as that of the fundamental structure along the  $a$ - and  $b$ -axes, and three times that along the  $c$ -axis for  $x = 8/7$  [10–12]. The tetragonal PbO-type  $\alpha\text{-FeSe}$  phase has an Fe-based planar sublattice equivalent to layered Fe-based oxypnictides, which have a layered crystal structure belonging to the  $P4/nmm$  space group. A crystal of  $\alpha\text{-FeSe}$  is composed of a stack of edge-sharing  $\text{FeSe}_4$  tetrahedra layer by layer [6]. Until now, research on  $\alpha\text{-FeSe}$  has mostly concentrated on polycrystal samples, and it is difficult to get a pure FeSe phase polycrystal sample using the technology reported in [6]. Therefore, a single crystal sample of FeSe is an particular requirement for the study of superconducting and structural transformation properties.

In this work, we have grown crystals of  $\text{FeSe}_x$  by the flux method using NaCl/KCl as the flux in an evacuated sealed

<sup>1</sup> Author to whom any correspondence should be addressed.

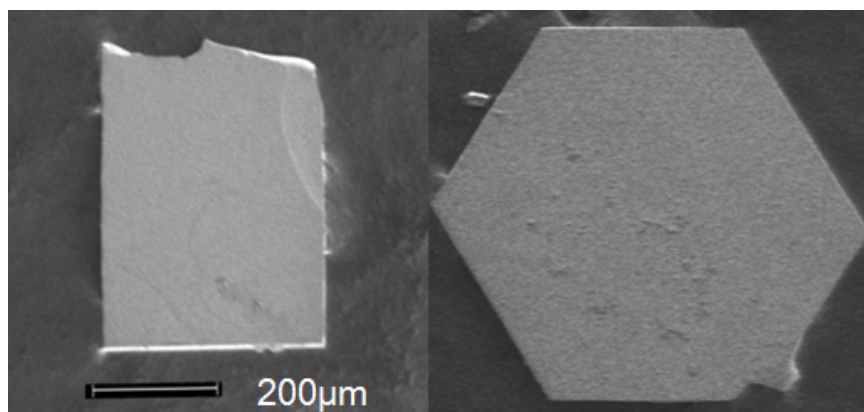


Figure 1. Photographs of  $\text{FeSe}_x$  crystals with different shapes.

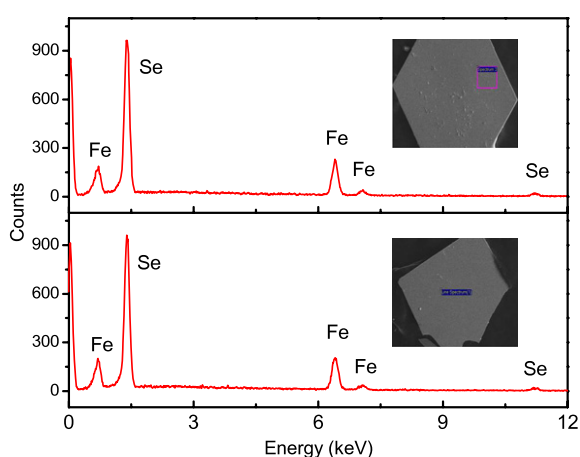


Figure 2. Energy dispersive x-ray spectrum (EDS) of  $\text{FeSe}_x$  crystals with different phases.

quartz tube. The structural, electronic transport, and magnetic properties have been studied to characterize the crystals.

## 2. Experimental procedure

Crystals of  $\text{FeSe}_x$  were grown using a high-temperature flux method in an evacuated sealed quartz tube. First,  $\text{FeSe}_{0.82}$  polycrystal powder was prepared by the method reported in [6] using high-purity powders of appropriate selenium and iron stoichiometry as raw materials. The obtained  $\text{FeSe}_{0.82}$  powders with several times of flux (NaCl/KCl 1/1: mol ratio) were ground and sealed in an evacuated quartz tube. The quartz tube was placed inside a vertical resistance furnace and heated to a final temperature of 850 °C. A soak time of 2 h was used to ensure sufficient solution of the raw materials. Then the furnace was cooled at a rate of 3 °C h<sup>-1</sup> to 600 °C. Finally, the furnace was cooled rapidly to room temperature to avoid possible twinning. The  $\text{FeSe}_x$  crystals were separated from the flux by dissolving the NaCl/KCl in deionized water.

The crystal structures were determined by x-ray diffraction (XRD) using a Philips X'pert PRO x-ray diffractometer with Cu  $K\alpha$  radiation at room temperature. The resistance measurement was performed by the standard four-

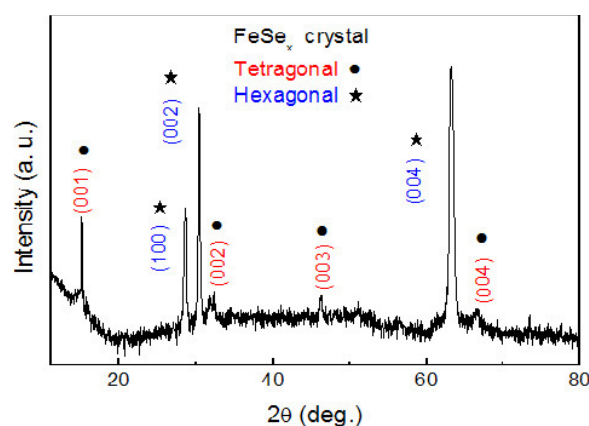


Figure 3. XRD pattern from several flakes of  $\text{FeSe}_x$ .

probe method using a Quantum Design physical property measurement system (PPMS) (1.8 K  $\leq T \leq$  400 K, 0 T  $\leq H \leq$  9 T). Magnetization measurements as a function of temperature were performed in a Quantum Design superconducting quantum interference device (SQUID) system (1.8 K  $\leq T \leq$  400 K, 0 T  $\leq H \leq$  5 T).

## 3. Results and discussion

### 3.1. Phase and structure analysis

The obtained crystals are black and mirror-like, with a typical size of  $0.5 \times 0.5 \times 0.03 \text{ mm}^3$ . Some flakes are rectangular, while other flakes are hexagonal. Figure 1 shows typical photographs of  $\text{FeSe}_x$  crystals with two different shapes. The estimated molar ratio of Fe:Se is about 1:1 by energy dispersive x-ray spectrum (EDS) analysis; the results are given in figure 2.

Because the size of the  $\text{FeSe}_x$  crystals is very small, we chose several flakes of  $\text{FeSe}_x$  for the  $2\theta$  XRD analysis, and show the results in figure 3. The XRD results show that the samples have two crystal structures, tetragonal and hexagonal, with space groups  $P4/nmm$  and  $P6_3/mmc$ . This result corresponds to the shapes of the  $\text{FeSe}_x$  crystal flakes. It is suggested that both tetragonal and hexagonal phase  $\text{FeSe}_x$  crystals can be grown by this method. The calculated lattice

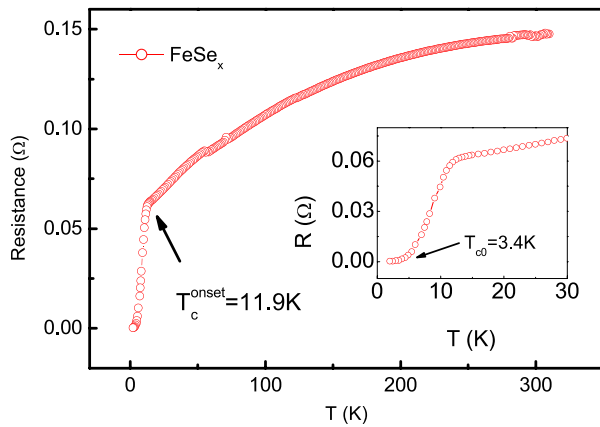


**Figure 4.** Temperature dependence of resistance of  $\text{FeSe}_x$  crystal at zero field. The inset is a magnified plot of resistance in the low-temperature region.

constant is  $c = 5.8747 \text{ \AA}$ , using the  $2\theta$  data for the (00 $l$ ) peak for tetragonal  $\text{FeSe}_x$  crystals, which is larger than  $c = 5.4861 \text{ \AA}$  reported before [6], [13]. And according to the  $2\theta$  data for the ( $h00$ ) and (00 $l$ ) peaks for hexagonal  $\text{FeSe}_x$  crystals, the lattice constants are  $a = b = 3.1168 \text{ \AA}$ ,  $c = 5.8839 \text{ \AA}$ .

### 3.2. Superconductivity

The resistance measurement was performed with the standard four-probe method using the PPMS. First, the sample was put on a copper flake with insulating glue. Then the epoxy was used to adhere a gold line (diameter  $25 \mu\text{m}$ ) to the crystal sample as probes under a microscope. Then, the product was annealed for 2 h in an Ar flow to volatilize the organic compound in the epoxy. Finally, the product was linked to the equipment by silver glue for measurement on the PPMS. The resistance shows an increase after the annealing.

The temperature dependence of resistance in the  $ab$  plane ( $2 \text{ K} < T < 310 \text{ K}$ ) under zero field for the  $\text{FeSe}_x$  crystal is plotted in figure 4. As can be seen, the  $\text{FeSe}_x$  crystal has a metallic behavior in the normal state. The resistance has a quick drop below the onset temperature of about  $T_c^{\text{onset}} = 11.9 \text{ K}$ , and zero resistance is attained below  $3.4 \text{ K}$ , indicating that superconductivity was indeed realized in this system. The superconducting transition width (10%–90%) is about  $8 \text{ K}$ . The larger transition width is possibly attributed to the slight oxidation when the crystals are annealed in the Ar flow. There is no obvious abnormality at  $\sim 100 \text{ K}$ , where  $\text{FeSe}$  has a structural transition, reported previously [6, 9]. It is suggested that the structural transition has little influence on the electronic transport properties of  $\text{FeSe}_x$  crystals.

A single flake of  $\text{FeSe}_x$  is very small, so we chose several flakes for the magnetic measurement. Figure 5 shows the temperature dependence of the dc magnetic susceptibility for  $\text{FeSe}_x$  crystal under a 10 Oe field. A sharp drop indicating the onset of superconductivity appearing at  $\sim 10.4 \text{ K}$  is observed for zero-field-cooling (ZFC) measurements, which further confirms the existence of superconductivity. And we note that the field-cooling (FC) measurements have a relatively large

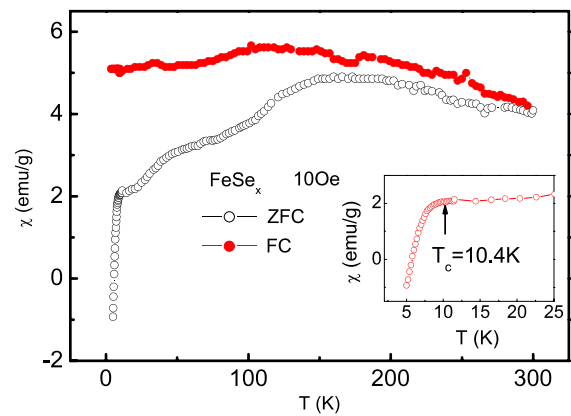


**Figure 5.** Temperature dependence of magnetic susceptibility  $\chi(T)$  for  $\text{FeSe}_x$  crystals at 10 Oe. The inset is a magnified plot of  $\chi(T)$  in the low-temperature region.

positive magnetic susceptibility below  $T_c$ . This is suggested to be related to the unsuperconductive  $\text{FeSe}_x$  phase in the magnetic measurement sample. And in the normal state, there are two obvious magnetic abnormalities that occur at 30 and 100 K, and the abnormality at 105 K is also pronounced in the field-cooling measurement. This abnormality suggested that the  $\text{FeSe}_x$  crystal has a structural transition at about 100 K, in accordance with previous reports [6, 9].

## 4. Conclusions

In summary,  $\text{FeSe}_x$  crystals were successfully grown in an evacuated sealed quartz tube using a NaCl/KCl flux. Structure analysis shows that the product has two crystal structures: (1) tetragonal,  $P4/nmm$ , and (2) hexagonal,  $P6_3/mmc$ . The results of resistivity and magnetization measurements clearly show that  $\text{FeSe}_x$  becomes a superconductor below  $\sim 10 \text{ K}$ .

## Acknowledgments

This work was supported by the National Key Basic Research under contract Nos 2006CB601005, 2007CB925002, and the National Nature Science Foundation of China under contract Nos 10774146, 10774147 and Director's Fund of Hefei Institutes of Physical Science, Chinese Academy of Sciences.

## References

- [1] Kamihara Y, Watanabe T, Hirano M and Hosono H 2008 *J. Am. Chem. Soc.* **3296** 130
- [2] Chen X H, Wu T, Wu G, Liu R H, Chen H and Fang D F 2008 *Nature* **453** 761
- [3] Chen G F, Li Z, Wu D, Li G, Hu W Z, Dong J, Zheng P, Luo J L and Wang N L 2008 *Phys. Rev. Lett.* **100** 247002
- [4] Ren Z A *et al* 2008 *Europhys. Lett.* **82** 57002
- [5] Hsu F C *et al* 2008 arXiv:0807.2369 [cond-mat]
- [6] Fang L, Yang H, Cheng P, Zhu X, Mu G and Wen H-H 2008 arXiv:0803.3978v1
- [7] Mizuguchi Y, Tomika F, Tsuda S, Yamaguchi T and Takano Y 2008 arXiv:0807.4315
- [8] Li L, Yang Z R, Ge M, Pi L, Xu J T, Wang B S, Sun Y P and Zhang Y H 2008 arXiv:0809.0128

- [9] Margadonna S, Takabayashi Y, McDonald M T, Kasperkiewicz K, Mizuguchi Y, Takano Y, Fitch A N, Suard E and Prassides K 2008 arXiv:[0807.4610](https://arxiv.org/abs/0807.4610)
- [10] Okazaki A and Hirakawa K 1956 *J. Phys. Soc. Japan* **11** 930
- [11] Okazaki A 1959 *J. Phys. Soc. Japan* **14** 112
- [12] Okazaki A 1961 *J. Phys. Soc. Japan* **16** 1162